

https://doi.org/10.1070/QEL16475

Broadband mid-IR difference-frequency generation in 5 mol % MgO-doped periodically and aperiodically poled lithium niobate

Jiandong Zhang, Jian Jiang, Kai Wang, Xuan Xiao, Siyao Yu, Zuxing Zhang

Abstract. **We have theoretically investigated broadband mid-infrared (mid-IR) difference-frequency generation (DFG) in 5 mol % MgO-doped periodically poled lithium niobate (5 mol % MgO : PPLN) based on quasi-phase-matching (QPM) with group-velocity matching (GVM) between the pump and the idler for the eee interaction of QPM. The acceptance bandwidths are 282.3 nm and 35.4 nm around 3.4 μm with the signal and pump wavelengths fixed at 1.550 μm and 1.064 μm, and the required QPM periods are 30.26 μm and 30.25 μm, respectively. A method which can broaden the flattop QPM DFG acceptance bandwidth (ABW) around the GVM wavelength for the idler wavelength in 5 mol % MgO-doped aperiodically poled lithium niobate (5 mol % MgO : APPLN) is proposed. The structure of 5 mol % MgO : APPLN is optimised using a genetic algorithm by adjusting its parameters. The simulation results show that under the GVM conditions, the maximum ABW for the idler is 1045.9 nm and 96.6 nm at a fixed signal wavelength of 1.550 μm and at a fixed pump wavelength of 1.064 μm, respectively. The tradeoff between the reduced effective nonlinear coefficient and DFG ABW is discussed.**

Keywords: *broadband difference-frequency generation, group-velocity matching, aperiodically poled crystal.*

1. Introduction

Mid-infrared (mid-IR) lasers are widely used in trace-gas detection, spectroscopy, optical sensing and detection [1, 2]. It is important that the acceptance bandwidth (ABW) of mid-IR lasers should be as large as to meet the characteristic absorption of some of the most important gas molecules in the spectral between 3 and 5 μm. In 2016, Masashi Abe et al. [3] obtained a quasi-phase-matching (QPM) ABW over 100 nm for the idler wavelength around 3.3 μm by using difference-frequency generation (DFG) in a periodically poled $LiNbO_3$ (PPLN) as a nonlinear crystal. This DFG source was then utilised to evaluate the temperature dependence of absorbance of gaseous methane. This suggests that the DFG technique is promising for broadening the DFG idler spectral region [4]. However, for normal periodically poled crystals, the QPM ABW for the idler wavelength range is only 1–10 cm^{-1} [5]. Therefore, the ABW of the QPM nonlinear poled crystal for a mid-IR DFG laser source should be broadened to meet some certain applications.

Some approaches have already proposed to increase the QPM ABW for the idler, such as phase modulation [6], chirping [7], group-velocity matching (GVM) [8, 9]. Besides, a QPM idler wavelength tuning range from 3300 nm to 3478 nm for a DFG mid-IR laser source has been experimentally demonstrated by exploiting the index dispersion of the nonlinear crystal with a fibre laser as a fundamental source [10]. Additionally, the temperature gradient control is also an effective method to increase the QPM DFG ABW for the idler [11, 12]. However, it is difficult to broaden the ABW of the idler while preserving the flattop conversion efficiency.

In this paper, we continue our theoretical investigation of broadband QPM DFG in 5 mol % MgO : PPLN with the GVM between the pump (signal) and idler under conditions when the signal (pump) wavelength is fixed by using the index dispersion of the nonlinear crystal. Then, we put forward a method to broaden the flattop QPM DFG ABW for the idler based on an aperiodically domain-inverted poled crystal. In our study, a genetic algorithm [13] is applied to optimise the required aperiodic structure of 5 mol % MgO-doped aperiodically poled $LiNbO_3$ (5 mol % MgO : APPLN) by adjusting the position and number of the pump (signal) wavelength at a fixed signal (pump) wavelength. Furthermore, the tradeoff between the reduced effective nonlinear coefficient and DFG ABW is also discussed.

2. Theory for broadband QPM DFG

QPM is an important technique in frequency conversion [14, 15]. In a so-called small signal approximation, as for DFG, the idler conversion efficiency based on QPM is proportional to $[\sin(\Delta k_{\mathrm{QPM}}L/2)/(\Delta k_{\mathrm{QPM}}L/2)]^2$ [16], where L is the length of the nonlinear crystal;

$$\Delta k_{\mathrm{QPM}} = \Delta k - \boldsymbol{G} = 2\pi\left(\frac{n_{\mathrm{p}}}{\lambda_{\mathrm{p}}} - \frac{n_{\mathrm{s}}}{\lambda_{\mathrm{s}}} - \frac{n_{\mathrm{i}}}{\lambda_{\mathrm{i}}} - 1/\Lambda\right) \tag{1}$$

is the overall phase mismatch; Δk is the phase mismatch; $\boldsymbol{G}$ is the reciprocal vector of the nonlinear crystal structure; Λ is the QPM period of the nonlinear crystal; and $\lambda_{\mathrm{p,s,i}}$ and $n_{\mathrm{p,s,i}}$ are the wavelengths and refractive indices of the pump, signal and idler, respectively. Here $\lambda_{\mathrm{p,s,i}}$ should satisfy the well-known energy conservation law: $1/\lambda_{\mathrm{p}} - 1/\lambda_{\mathrm{s}} - 1/\lambda_{\mathrm{i}} = 0$.

Jiandong Zhang, Kai Wang, Xuan Xiao, Siyao Yu School of Opto-electronic Engineering, Nanjing University of Posts and Telecommunications, Nanjing 210023, China;
Jian Jiang, Zuxing Zhang Advanced Photonics Technology Laboratory, Nanjing University of Posts and Telecommunications, Nanjing 210023, China; e-mail: jiangjian@njupt.edu.cn, zxzhang@njupt.edu.cn

Received 13 July 2017; revision received 12 December 2017
Kvantovaya Elektronika **48** (3) 222–227 (2018)
Submitted in English

Differentiating Δk_{QPM} (1) with the idler angular frequency ω_i for the fixed signal frequency ω_s, we obtain:

$$\frac{d\Delta k_{QPM}}{d\omega_i} = \frac{d\Delta k}{d\omega_i} - \frac{d(2\pi/\Lambda)}{d\omega_i},$$

with the first term written as [17]:

$$\frac{d\Delta k}{d\omega_i} = \frac{d(k_p - k_s - k_i)}{d\omega_i} = \frac{dk_p}{d\omega_i} - \frac{dk_i}{d\omega_i}$$
$$= \frac{dk_p}{d\omega_p} - \frac{dk_i}{d\omega_i} = \frac{1}{v_{gp}} - \frac{1}{v_{gi}}, \quad (2)$$

where v_{gp} and v_{gi} are the group velocities of the pump and idler waves, respectively. The GVM condition $v_{gp} = v_{gi}$ can be met in the spectral region, where Δk_{QPM} takes an extremum, $d\Delta k_{QPM}/d\omega_i = 0$, around which the broadband QPM DFG can be obtained over a wide wavelength range.

We assume that all the waves propagate along z axes. Then, the coupled wave equations of the three waves have the form [18]:

$$\frac{\partial E_p}{\partial z} = -\frac{i\omega_p d_{33}}{n_p c}\tilde{d}(z)E_s^* E_i \exp(-i\Delta kz), \quad (3a)$$

$$\frac{\partial E_s}{\partial z} = -\frac{i\omega_s d_{33}}{n_s c}\tilde{d}(z)E_p^* E_i \exp(-i\Delta kz), \quad (3b)$$

$$\frac{\partial E_i}{\partial z} = -\frac{i\omega_i d_{33}}{n_i c}\tilde{d}(z)E_p E_s \exp(i\Delta kz), \quad (3c)$$

where E_t (t = p, s, i) is the envelope of the electric field intensity; d_{33} is the nonlinearity coefficient; $\tilde{d}(z)$ takes the values of ± 1 and characterises the orientation of each polarised poled structure; and $\Delta k = k_p - k_s - k_i$. Then, we integrate formula (3c) along the length L of the crystal and obtain:

$$E_i(z = L) = \frac{i\omega_i}{n_i c} d_{33} E_p E_s L d(\lambda), \quad (4)$$

where

$$d(\lambda) = \frac{1}{L}\int_0^L \tilde{d}(z)\exp(i\Delta kz)\,dz.$$

Thus, the DFG conversion efficiency reads:

$$\eta_{DFG} = \frac{8\pi^2 d_{33}^2 L^2 I_p}{n_p n_s n_i \lambda_i^2 c\varepsilon_0}\left|\frac{1}{L}\int_0^L \tilde{d}(z)\exp(i\Delta kz)\,dz\right|^2$$
$$= \frac{8\pi^2 d_{33}^2 L^2 I_p}{n_p n_s n_i \lambda_i^2 c\varepsilon_0}\left|d_{reff}(\lambda)\right|^2, \quad (5)$$

where I_p is the pump intensity. To simply the problem of designing an aperiodically poled nonlinear crystal structure, we consider the last term

$$d_{reff}(\lambda) = \left|\frac{1}{L}\int_0^L \tilde{d}(z)\exp(i\Delta kz)\,dz\right|$$

in Eqn (5), which, with an accuracy to a constant term, determines the DFG efficiency and is called the reduced effective nonlinear coefficient [19]. If the nonlinear crystal is equally divided into N block with the same length of each blocks ΔL, we obtain [20]:

$$d_{reff}(\lambda) = \left|\frac{1}{L}\int_0^L \tilde{d}(z)\exp(i\Delta kz)\,dz\right|$$
$$= \frac{1}{L}\left|\sum_{q=0}^{N-1}\tilde{d}(z)\int_{z_q}^{z_{q+1}}\exp(i\Delta kz)\,dz\right|$$
$$= \frac{1}{L}\left|\sum_{q=0}^{N-1}\tilde{d}(z)\frac{\exp(i\Delta kz_{q+1}) - \exp(i\Delta kz_q)}{i\Delta k}\right|$$
$$= \frac{1}{L\Delta k}\left|\sum_{q=0}^{N-1}\tilde{d}(z)[\exp(i\Delta kz_{q+1}) - \exp(i\Delta kz_q)]\right|. \quad (6)$$

The position of each block is located between the coordinates z_q and z_{q+1} ($q = 0, 1, 2, 3, ..., N$). The desired structure of the aperiodically polded crystal will be obtained by optimising $\tilde{d}(z)$, and the QPM DFG conversion efficiency can be obtained by substituting $\tilde{d}(z)$ into Eqn (5).

3. Simulations and discussion

In the simulations, we used a crystal with a length of 10 mm. The refractive indices $n_{p,s,i}$ are a function of wavelength and temperature; this dependence can be calculated by the Sellmeier equation [21]. The QPM DFG ABW for the idler is defined as the full width at half maximum (FWHM) of the normalised conversion efficiency.

For the eee interaction under conditions of QPM DFG in 5 mol % MgO:PPLN with a fixed signal wavelength of 1.550 μm, Fig. 1 shows the group-velocity mismatch and the QPM periods as a function of idler wavelength with a temperature set at 120°C. One can see from Fig. 1 that the GVM idler wavelengths are located at 3.403 μm where the group velocity of the idler is equal to that of the pump. The corresponding QPM period is 30.26 μm which is calculated from

$$\Lambda = 1/(n_p/\lambda_p - n_s/\lambda_s - n_i/\lambda_i).$$

Then the QPM DFG ABW is calculated from

$$[\sin(\Delta k_{QPM}L/2)/(\Delta k_{QPM}L/2)]^2$$

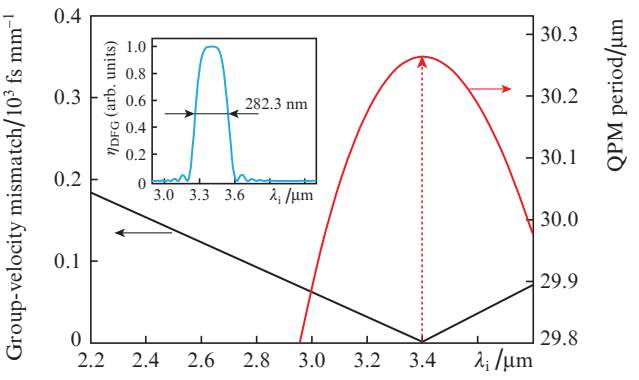

Figure 1. Group-velocity mismatch and QPM period vs. idler wavelength λ_i for eee QPM. The inset shows the normalised DFG conversion efficiency η_{DFG} at the GVM wavelength.

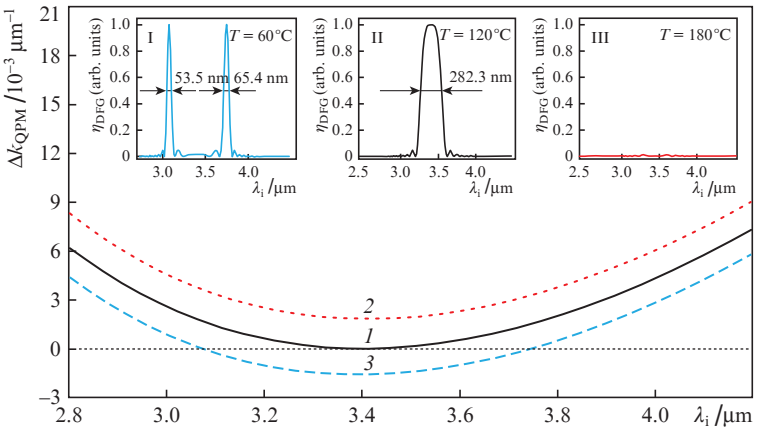

Figure 2. Phase mismatch as a function of idler wavelength λ_i at temperatures T = (*3*) 60°C, (*1*) 120°C, and (*2*) 180°C. The insets show the normalised DFG conversion efficiency η_{DFG} at the corresponding temperatures with the QPM period fixed at Λ = 30.26 μm.

at the GVM wavelength. As shown in the inset of Fig. 1, a broad bandwidth of 282.3 nm can be obtained at 3.403 μm.

Figure 2 shows the dependence of the phase mismatch on the idler wavelength at temperatures T = 60°C, 120°C, and 180°C. The insets illustrate the normalised conversion efficiency at the corresponding temperature with a QPM period fixed at Λ = 30.26 μm. The horizontal dashed line which represents $\Delta k_{QPM} = 0$ is tangent to the phase-mismatch curve at a wavelength of 3.403 μm for the temperature of 120°C [curve (*1*)], where the conversion efficiency can be obtained with the QPM and GVM conditions satisfied simultaneously (see inset II in Fig. 2). Obviously, curve (*1*) will shift upward [curve (*2*)] or downward [curve (*3*)] as the temperature changes. Curve (*3*) which represents the phase mismatch at 60°C intersects the horizontal line at 3.074 μm and 3.747 μm with the same value of Δk = 0.2076 μm^{-1}, where two reciprocal vectors are provided by the nonlinear crystal to satisfy the QPM condition ($\Delta k_{QPM} = \Delta k - 2\pi/\Lambda = 0$) without GVM. Thus two QPM DFG bands with the ABW of 53.5 nm and 65.4 nm can be obtained at these two wavelengths (see inset I in Fig. 2). However, when the temperature is higher than 120°C, the horizontal line no longer intersects the curve. In this situation, neither QPM nor GVM condition can be satisfied, and the conversion efficiency is almost zero (see inset III in Fig. 2).

It follows from the above data that that the broadband DFG ABW is around 3.403 μm at 120°C due to intrinsic dispersion properties of the crystal in question, and the idler ABW evolves to two separate QPM bands as the temperature gradually decreases. Now we calculate the idler ABW on the right side of 3.403 μm (Fig. 3). The calculations show that the ABW decreases with decreasing temperature, for example, when the temperature is set at 100°C, 60°C, and 20°C, the ABWs are 109.3, 65.4, and 53.2 nm, respectively (see the inset in Fig. 3).

The reasons for the bandwidth to become larger are given below. Figure 4 shows the phase mismatch as a function of idler wavelength at different temperatures when the signal wavelength is fixed at 1.550 μm. One can see that the region of the phase mismatch which satisfies the FWHM condition for $[\sin(\Delta k_{QPM}L/2)/(\Delta k_{QPM}L/2)]^2$ is located between the horizontal dashed lines (*1*) and (*2*), which correspond to $\Delta k_{QPM} = \pm 0.2783 \times 10^{-3}$ μm^{-1}. Because lines (*1*) and (*2*) are rather close to each other, the wavelength dependence of the phase mismatch in this interval can be approximately regarded as a

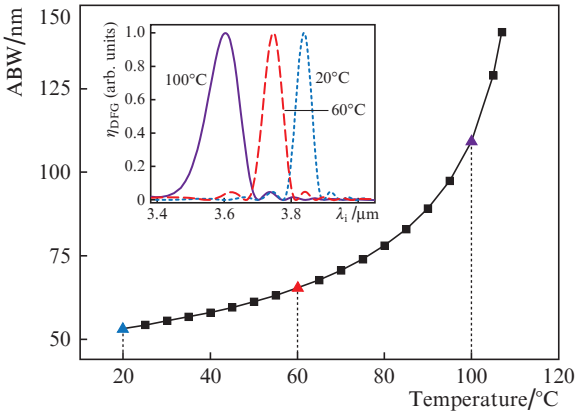

Figure 3. ABW in the case of the idler wavelength (λ_i) detuning from the GVM wavelength as a function of temperature. The inset shows the DFG conversion efficiency η_{DFG} at different temperatures.

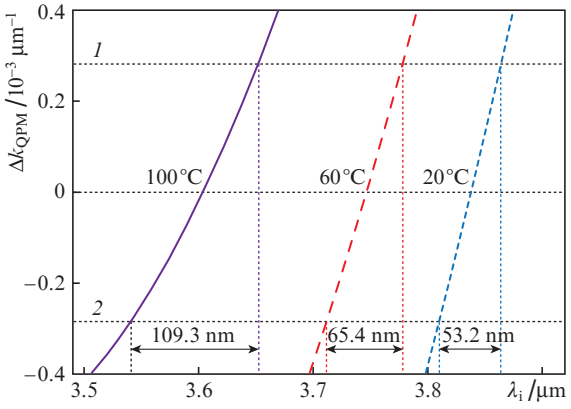

Figure 4. Phase mismatch under QPM as a function of idler wavelength λ_i for different temperatures.

straight line; therefore, the lower the temperature of the crystal, the smaller the slope, which means that the bandwidth would decrease with decreasing temperature.

Figure 5 shows the conversion efficiency and QPM period as a function of idler wavelength at a pump wavelength fixed

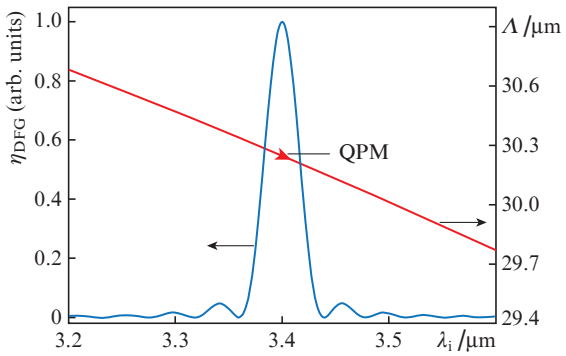

Figure 5. Normalised DFG conversion efficiency η_{DFG} and QPM period Λ as functions of idler wavelength λ_i.

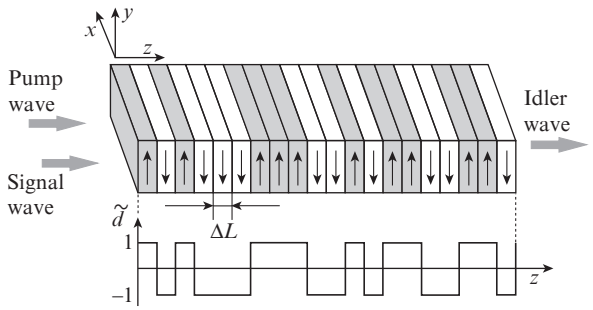

Figure 6. Schematic of the 5 mol % MgO : APPLN crystal.

at 1.064 μm. The QPM period required for broadband DFG at the idler wavelength of 3.403 μm is 30.25 μm at a temperature of 120°C. In this case, the ABW for QPM DFG is 35.4 nm.

Thus, the emergence of reciprocal vectors from a periodically poled crystal is limited by the temperature and QPM period, which leads to a considerable restriction of the ABW broadening. To solve this problem, we have designed a domain-inverted aperiodically poled crystal which can compensate for the wave vector mismatch and thus effectively broaden the QPM DFG ABW for the idler. To this end, the aperiodically poled crystal structure is designed with a genetic algorithm (GA) to broaden the ABW of QPM DFG [22, 23].

The 5 mo l % MgO : APPLN crystal with a total length of about 10 mm is divided into 3333 uniform domains with the domain width chosen at 3 μm for ease of fabrication. Thus, the algorithm needs to search for the optimal structure from the 2^{3333} variants. The scheme of the algorithm is as follows. First, a randomly generated initial population of P(0) is composed of $J = 200$ individuals. Each individual consists of 3333 genes expressed as two binary values of $\tilde{d}(z) = \pm 1$, with 1 representing positively polarised domains and –1 representing negatively polarised domains, respectively. Thus, each individual can represent one type of an aperiodically poled structure. Second, to optimise the domain distribution function $\tilde{d}(z)$ by the GA, the overall reduced effective nonlinear coefficient

$$\sum_{j=1}^{M} d_{\mathrm{reff}}(\lambda_j) = \sum_{j=1}^{M} \left| \frac{1}{L} \int_0^L \tilde{d}(z) \exp(\mathrm{i}\Delta k z)\, \mathrm{d}z \right|$$

is chosen as the objective function, where M is the number of the pump (signal) wavelengths and Δk is calculated according to the designed wavelengths. Meanwhile, to maximise the efficiency and make the top of the efficiency curve flat, we introduce the fitness function

$$\sigma_{\mathrm{fit}} = \sqrt{\frac{1}{M} \sum_{j=1}^{M} \left[d_{\mathrm{reff}}(\lambda_j) - \sum_{j=1}^{M} d_{\mathrm{reff}}(\lambda_j)/M \right]^2}.$$

The smaller the value of σ_{fit}, the greater the value of fitness. Then, a series of standard functions of the GA, such as selection, crossover and mutation, are performed on P(Q) to generate a set of off-springs Φ. Next, a new population P(Q + 1) is generated by replacing some individuals of P(Q) with Φ, using the GA selection function reins( ). The procedure is repeated until the maximum number Q of generations reaches 500. Finally, an approximate optimal aperiodically poled structure $\tilde{d}(z)$ can be obtained by decoding the individual with the maximum fitness value in the final generation.

The schematic diagram of a 5 mol % MgO : APPLN crystal is shown in Fig. 6. The interface of each domain is parallel to the xy plane for using the largest nonlinear coefficient d_{33}. The incident light propagates along the z axis and the polari-

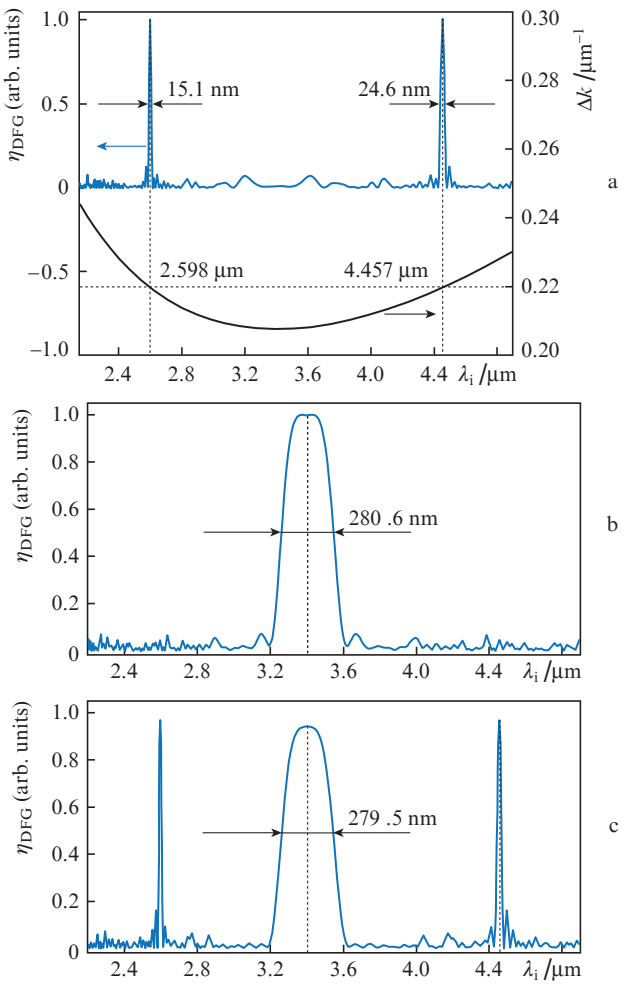

Figure 7. (a) Normalised conversion efficiency in an aperiodically poled crystal at a fixed pump wavelength of 1.150 μm and phase mismatch as functions of idler wavelength; (b, c) normalised conversion efficiency at a pump wavelength of 1.065 μm (b) or under simultaneous pumping at 1.065 and 1.150 μm (c).

sation direction coincides with the y axis. The arrows show the direction of up- and down-polarisation. The choice of polarisation is optimised by the genetic algorithm to obtain the best distribution of the modulated nonlinear coefficient. Then, the conversion efficiency is obtained after substituting the optimal domain structure functions $\tilde{d}(z)$ into Eqn (5).

The simulations were performed by choosing different positions and pump wavelengths. The normalised conversion efficiency and phase mismatch Δk as a function of idler wavelength is shown in Fig. 7a at a fixed signal wavelength of 1.550 μm. The wavelength of 1.150 μm is chosen as the pump wavelength. The simulation result shows that two QPM DFG bands with ABWs of 15.1 and 24.6 nm can be acquired at idler wavelengths of 2.598 and 4.457 μm, respectively, because these two positions have the same value of $\Delta k = 0.2198$ μm^{-1}. The same simulation results can be observed with the predesigned wavelengths of 0.971 and 1.150 μm. Then, we used a pump wavelength of 1.065 μm because the group velocity at this wavelength is equal to that of 3.403 μm. One can see from Fig. 7b that for the case under study the QPM DFG band of 280.6 nm can be obtained, which is almost the same as that for the periodically poled niobate crystal.

If two predesigned pump wavelengths of 1.065 and 1.150 μm are chosen simultaneously, three QPM DFG bands with ABWs of 15.2, 24.5 and 279.5 nm can be acquired but with only two predesigned pump wavelengths. Thus, the following simulations will be performed with a pump wavelength fixed at 1.065 μm and an additional pump having a slightly longer wavelength. Compared with the inset in Fig. 1, it is clear that crystals with an aperiodically inverted-domain structure can supply more reciprocal vectors flexible to match simultaneously more optical parametric processes; therefore, the QPM DFG ABW can be effectively broadened.

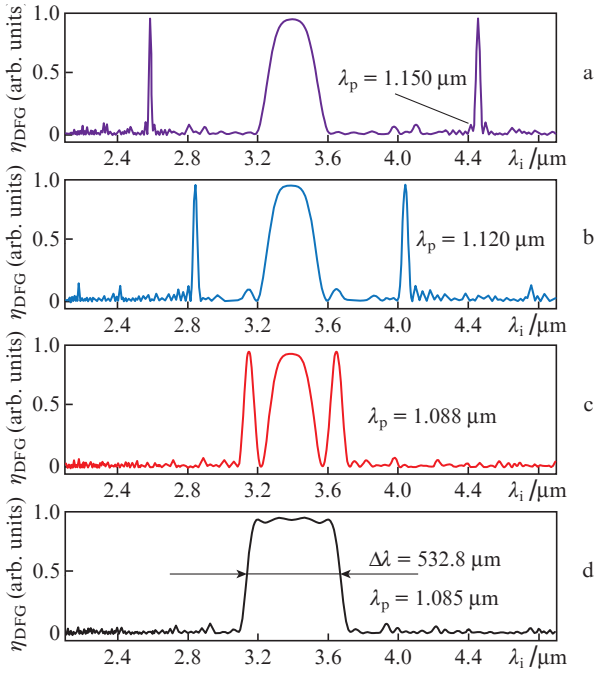

Figure 8. Normalised conversion efficiency for the idler wavelength at a fixed pump wavelength of 1.065 μm and an additional pump wavelength gradually shifting to it.

Figure 8 shows the simulations under pumping simultaneously at 1.065 μm and at a larger wavelength gradually shifting to it. As for the idler wavelength, it can be found that two narrow phase-matched bands become wider and wider as the additional pump wavelength moves towards 1.065 μm because of a decreasing slope of $\Delta k(\lambda)$. These changes are well observed in Figs 8a–8c. When the additional pump wavelength reaches 1.085 μm, the two idler wavelengths will near enough and a wide flattop QPM DFG band with the ABW of 532.8 nm is formed (see Fig. 8d).

In order to further broaden the QPM DFG ABW, the following simulations will be performed with pump wavelengths of 1.065 and 1.085 μm and with a pump wavelength added every 3 nm on the right side of 1.085 μm. Figure 9 shows the broadband QPM DFG obtained with the number of 1, 3, 6, 9 pump wavelengths added. The corresponding ABWs of QPM DFG are 555.3, 739.8, 837.5 and 1045.9 nm, respectively, with the reduced effective nonlinear coefficient $d_{reff}(\lambda)$ decreasing from 0.2373 to 0.2117, 0.1762, and 0.1533. One can see from Fig. 9 that the conversion efficiency decreases with increasing acceptance bandwidth. For a periodically poled structure of QPM, the effective nonlinear coefficient is $2d_{33}/\pi$, and the corresponding value of the effective nonlinear coefficient for the maximum bandwidth of 1045.9 nm is $d_{reff}(\lambda)d_{33} = 0.1533\,d_{33}$.

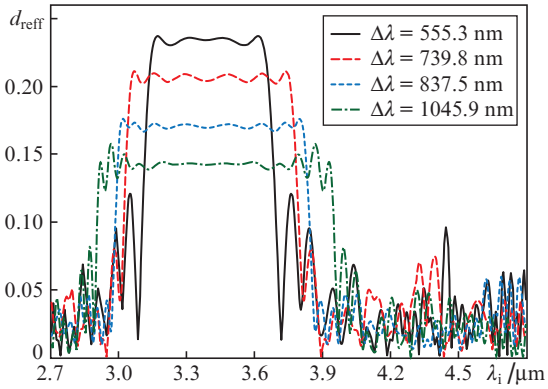

Figure 9. Reduced effective nonlinear coefficient for the idler wavelength at pump wavelengths of 1.065 and 1.085 μm and 1, 3, 6, and 9 pump wavelengths added every 3 nm on the right side of 1.085 μm.

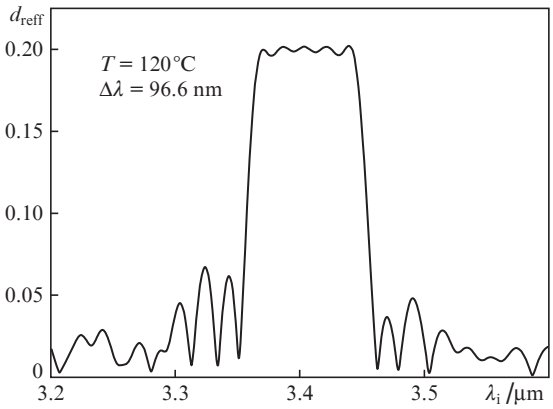

Figure 10. Reduced effective nonlinear coefficient for the idler wavelength at a fixed pump wavelength of 1.064 μm and a signal wave at different wavelengths.

In this case, the conversion efficiency ratio of periodically and aperiodically poled structures for the crystal in question is $(2d_{33}/\pi)^2/(d_{\text{reff}}\,d_{33})^2 \approx 17.25$; the acceptance bandwidth increases by approximately 3.7 times, while the conversion efficiency decreases to 5.80%.

Similarly, we optimised the aperiodically poled structure in the case of the fixed pump wavelength (1.064 μm) and signal wave at different wavelengths (in analogy with the previous case at a fixed signal wavelength). The maximal ABW for the aperiodically poled crystal was 96.6 nm at $d_{\text{reff}}(\lambda) = 0.2021$ (Fig. 10). Compared with a periodically poled structure, the bandwidth increases by 2.73 times with a decrease in the conversion efficiency to 10.08%.

4. Conclusions

We have theoretically analysed broadband mid-IR DFG in 5 mol % MgO : PPLN based on QPM with GVM between the pump and the idler for the eee interaction of QPM. The ABW of 282.3 nm around an idler wavelength of 3.403 μm is obtained under the corresponding QPM period of 30.26 μm at a temperature of 120°C in the case of a fixed signal wavelength of 1.550 μm. The conversion efficiency is calculated at different temperatures with this QPM period. The ABW of 96.6 nm around an idler wavelength of 3.403 μm is obtained under the corresponding QPM period of 30.25 μm at a fixed pump wavelength of 1.064 μm. A method is proposed to broaden the flattop QPM DFG ABW around the GVM idler wavelength based on an aperiodically poled lithium niobate crystal. An optimal aperiodically poled structure is obtained through the genetic algorithm. The simulation results show that the maximum QPM DFG ABW for the idler wavelength at a fixed signal wavelength of 1.550 μm (or a pump wavelength of 1.064 μm) is 1045.9 nm (96.6 nm) near a wavelength of 3.4 μm, which 3.7 (2.73) times greater than that for the periodically poled structure. However, compared with the periodically poled structure, the conversion efficiency decreases to 5.80% (10.08%).

Acknowledgements. This work was supported by the Natural Science Foundation of the Higher Education Institutions of Jiangsu Province, China (Grant No. 14KJB140010) and the Nanjing University of Posts and Telecommunications Foundation, China (Grant No. NY213029), the Jiangsu Specially Appointed Professor Project (Grant No. RK002STP14001) and the Six Talent bands Project in Jiangsu Province (2015-XCL-023).

References

1. Zhou S., Han Y.L., Li B.C. *Appl. Phys. B*, **122**, 187 (2016).
2. Northern J.H., O'Hagan S., Fletcher B., Gras B., Ewart P., Kim C.S., Kim M., Merritt C.D., Bewley W.W., Canedy C.L., Abell J., Vurgaftman I., Meyer J.R. *Opt. Lett.*, **40**, 4186 (2015).
3. Abe M., Nishida Y., Tadanaga O., Tokura A., Takenouchi H. *Opt. Lett.*, **41**, 1380 (2016).
4. Andreev A.L., Andreeva T.B., Kompanets I.N. *Quantum Electron.*, **41** (10), 881 (2011) [*Kvantovaya Elektron.*, **41** (10), 881 (2011)].
5. Chang J.H., Mao Q.H., Feng S.J., Gao X.M., Xu C.Q. *Opt. Lett.*, **35**, 3486 (2010).
6. Li B.H., Xu Y.G., Zhu H.F., Lin F.K., Li Y.F. *Phys. Rev. A*, **91**, 023827 (2015).
7. Yang J., Hu X.P., Xu P., Lv X.J., Zhang C., Zhao G., Zhou H.J., Zhu S.N. *Opt. Express*, **18**, 14717 (2010).
8. Lee K.J., Yoon C.S., Rotermund F. *Jpn. J. Appl. Phys.*, **44**, 1264 (2005).
9. Yu N.E., Ro J.H., Cha M., Kurimura S., Taira T. *Opt. Lett.*, **27**, 1046 (2002).
10. Jiang J., Chang J.H., Feng S.J., Wei L., Mao Q.H. *Opt. Express*, **18**, 4740 (2010).
11. Lee Y.L., Shin W., Yu B.A., Jung C., Noh Y.C., Ko D.K. *Opt. Express*, **18**, 7678 (2010).
12. Chang J.H., Yang Z.B., Sun Q. *Optik*, **126**, 1123 (2015).
13. Lai J.Y., Liu Y.J., Wu H.Y., Chen Y.H., Yang S.D. *Opt. Express*, **18**, 5328 (2010).
14. Zondy J.-J., Bonnin C., Lupinski D. *J. Opt. Soc. Am. B*, **20**, 1675 (2003).
15. Zondy J.-J., Bonnin C., Lupinski D. *J. Opt. Soc. Am. B*, **20**, 1695 (2003).
16. Yanagawa T., Kanbara H., Tadanaga O., Asobe M., Suzuki H., Yumoto J. *Appl. Phys. Lett.*, **86**, 161106 (2005).
17. Prakash O., Lim H.H., Kim B.J., Pandiyan K., Cha M., Rhee B.K. *Appl. Phys. B*, **92**, 535 (2008).
18. Shao G.H., Wu Z.J., Chen J.H., Xu F., Lu Y.Q. *Phys. Rev. A*, **88**, 063827 (2013).
19. Gu B.Y., Dong B.Z., Zhang Y., Yang G.Z. *Appl. Phys. Lett.*, **75**, 2175 (1999).
20. Lu M., Chen X.F., Chen Y.P., Xia Y.X. *Appl. Opt.*, **46**, 4138 (2007).
21. Gayer Q., Sacks Z., Galun E., Arie A. *Appl. Phys. B*, **91**, 343 (2008).
22. Haupt R.L., Haupt S.E. *Practical Genetic Algorithms* (New York: Wiley Press, 2004).
23. Conforti M., Baronio F., DeAngelis C., Sanna G., Pierleoni D., Bassi P. *Opt. Commun.*, **281**, 1693 (2008).